Supporting Information

Highly-Sensitive As^{3+} Detection Using Electrodeposited Nanostructured MnO_x and Phase Evolution of the Active Material During Sensing

Tanvi Gupte[a,b]‡, Sourav Kanti Jana[a]‡, Jyoti Sarita Mohanty[a], Pillalamarri Srikrishnarka[a], Sritama Mukherjee[a], Tripti Ahuja[a], Chennu Sudhakar[a], Tiju Thomas[b], Thalappil Pradeep[a]**

[a]DST Unit of Nanoscience (DST UNS) and Thematic Unit of Excellence, Department of Chemistry, Indian Institute of Technology Madras

[b]Department of Metallurgical and Materials Engineering, Indian Institute of Technology Madras

* Corresponding authors: pradeep@iitm.ac.in (Prof. T. Pradeep), tijuthomas@iitm.ac.in (Dr. Tiju Thomas)

‡These authors contributed equally.

TABLE OF CONTENTS

Figure/ Table No.	**Title**	**Page No.**
Table S1	Values of each component of the electronic circuit used to fit Nyquist plots of EIS for **M1**, **M2**, and **M3** electrodes	S3
Figure S1	Pourbaix (Eh-pH) diagram showing the predominant forms of manganese oxide and hydroxide	S4
Figure S2	FESEM micrographs of **M1** electrode	S5
Figure S3	FESEM micrographs of **M2** electrode	S6
Figure S4:	EDX spectra of **M3** electrode before (A) and after (B) As^{3+} sensing	S7
Figure S5	ICP-MS data for change in the arsenic and manganese ion concentrations before and after As^{3+} sensing of **M3** electrode	S8
Figure S6	TEM micrographs of **M1** electrode	S9
Figure S7	TEM micrographs of **M2** electrode	S10
Figure S8	XRD analysis of ITO glass substrate and control experiment on **M3** electrode	S11
Figure S9	XPS spectra of As 3d region	S12
Figure S10	Nyquist plot of bare ITO glass substrate	S13
Figure S11	Electrochemical arsenite sensing response by **M1** and **M2** electrodes	S14
Figure S12	CV of bare ITO at optimized parameters	S15
	Calculation of LOD	S16
References		S17

Table S1. Values of each component of the electronic circuit used to fit Nyquist plots of electrochemical impedance spectra (EIS) for **M1**, **M2**, and **M3** MnO_x/ITO electrodes. R1 is the internal resistance of the material, which directly influences the contact resistance between ITO and the electrodeposited material. R_{ct} is the charge transfer resistance at the electrode-electrolyte interface. Parallel combinations of both, C3-R3 and C4-R4 are related to diffusion of ions from the bulk electrolyte into porous network of the as-prepared electrode. Q1 and Q2 are called constant phase elements which are associated with the double layer capacitance formed in inter/intra particular porous structure.

	M1	**M2**	**M3**
R_S	47.2 Ω	72.5 Ω	58.2 Ω
Q1	$9*10^{-3}$ F.s $^{(a-1)}$	$0.2*10^{-3}$ F.s$^{(a-1)}$	$2*10^{-3}$ F.s$^{(a-1)}$
R_{ct}	121	26.3 Ω	21.8
C3	31.7 $*10^{-6}$ F	40.4 $*10^{-6}$ F	6.57 $*10^{-6}$ F
R3	1.12 KΩ	115.8 Ω	558.4 Ω
C4	1.9 $*10^{-9}$ F	1.7 $*10^{-9}$ F	$2.5*10^{-9}$ F
R4	54.07 Ω	66.3 Ω	119 Ω
Q2	$1.4*10^{-2}$ F.s $^{(a-1)}$	$0.2*10^{-3}$ F.s$^{(a-1)}$	1.3 $*10^{-2}$ F.s$^{(a-1)}$

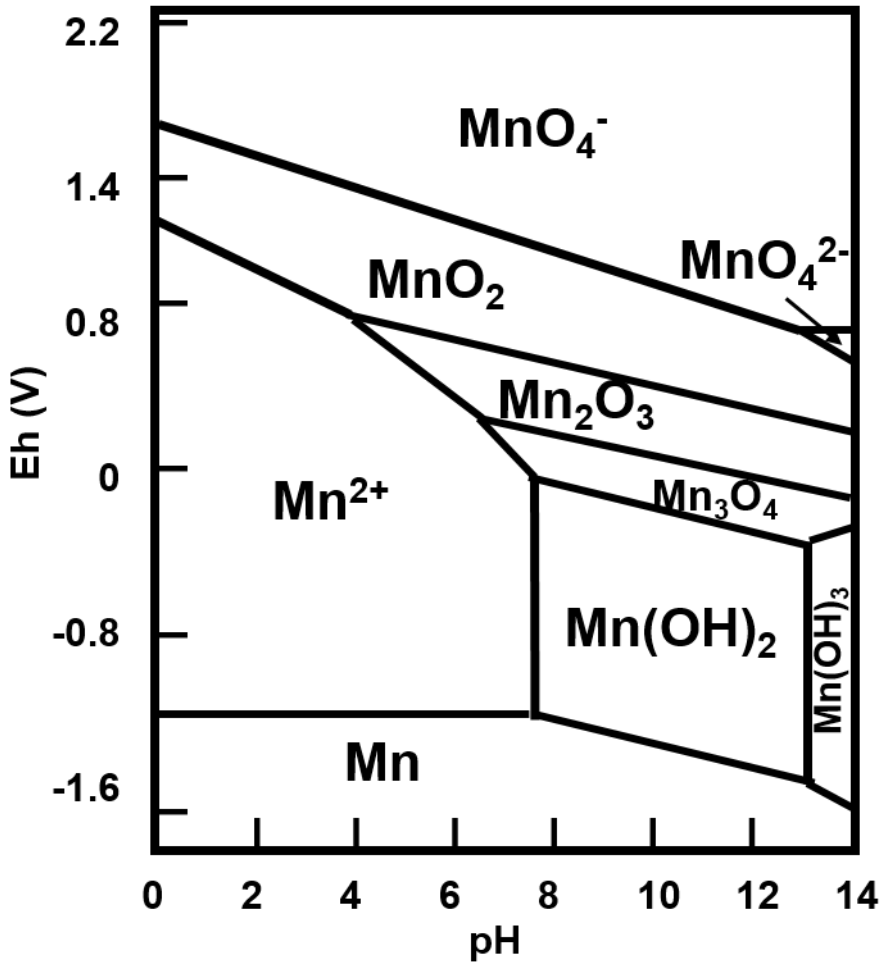

Figure S1. Pourbaix (Eh-pH) diagram showing the predominant forms of manganese oxide and hydroxide at 25°C ± 0.5.[1]

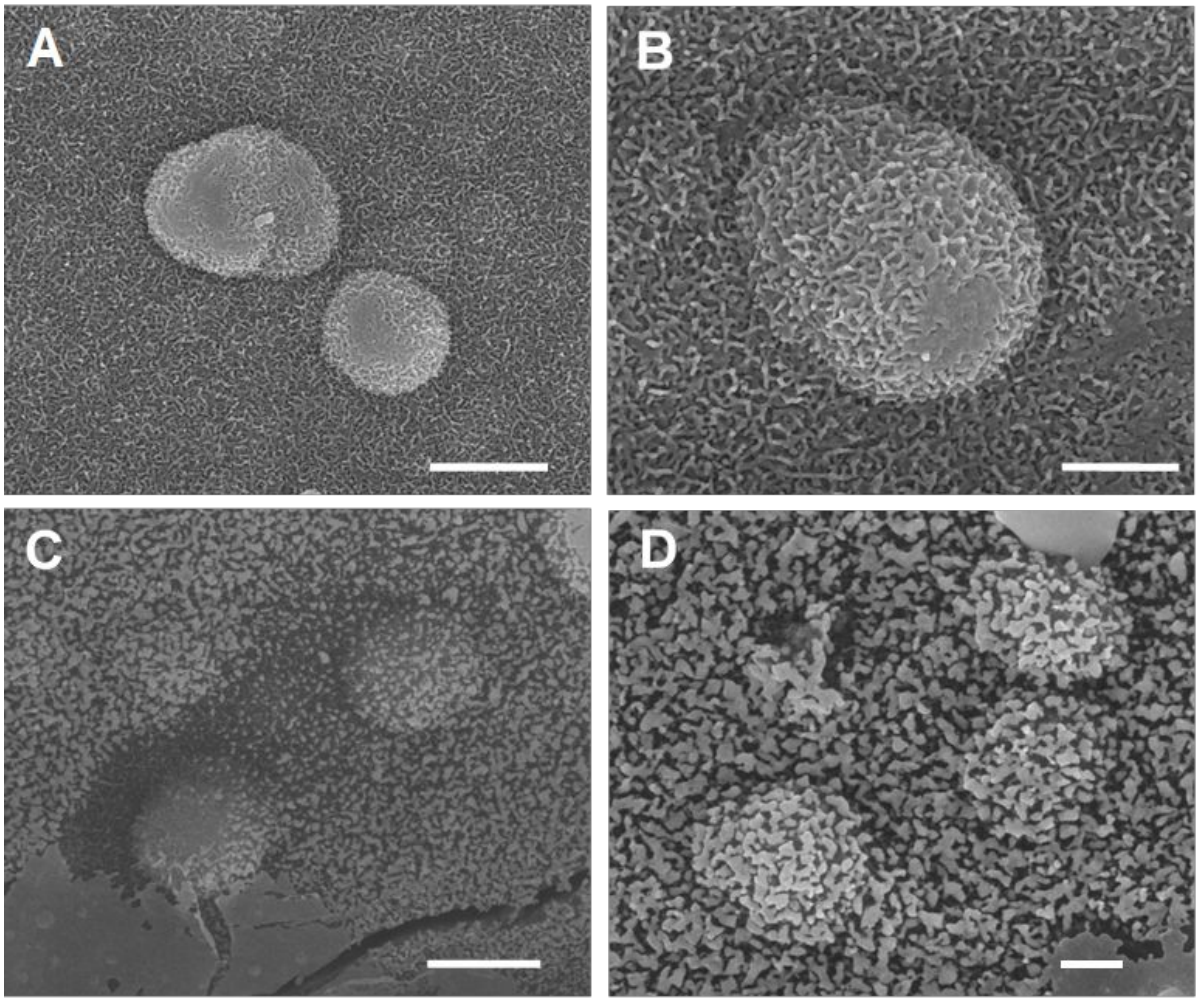

Figure S2. FESEM micrographs of (A and B) as-prepared **M1** MnO_x/ITO electrode and (C and D) after As^{3+} sensing. The scale bars are 1 μm for A and C, and 500 nm for B and D.

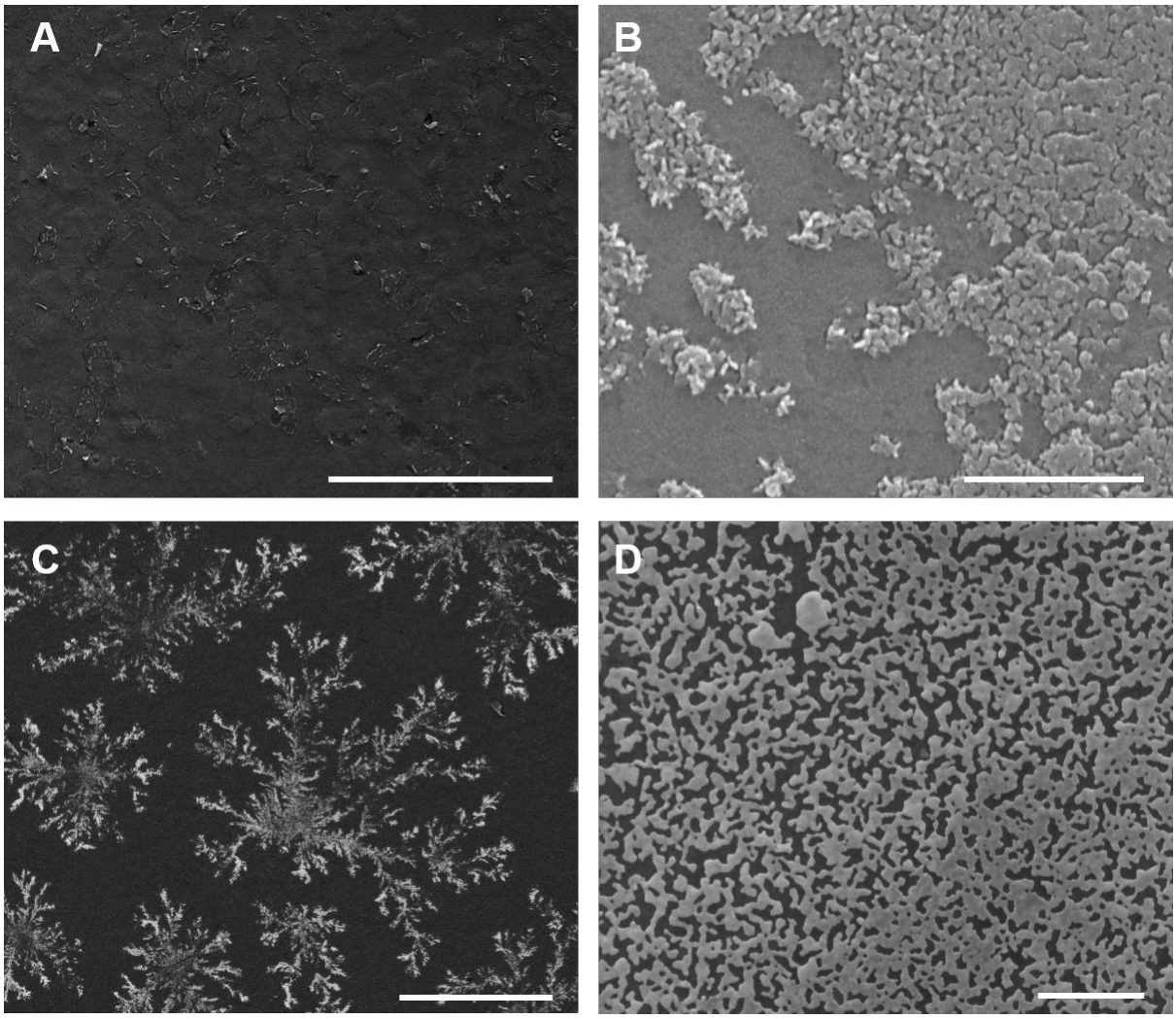

Figure S3. FESEM micrographs of (A and B) as-prepared **M2** MnO_x/ITO electrode and (C and D) after As^{3+} sensing. The scale bars are 100 μm for A and C, and 1 μm for B and D.

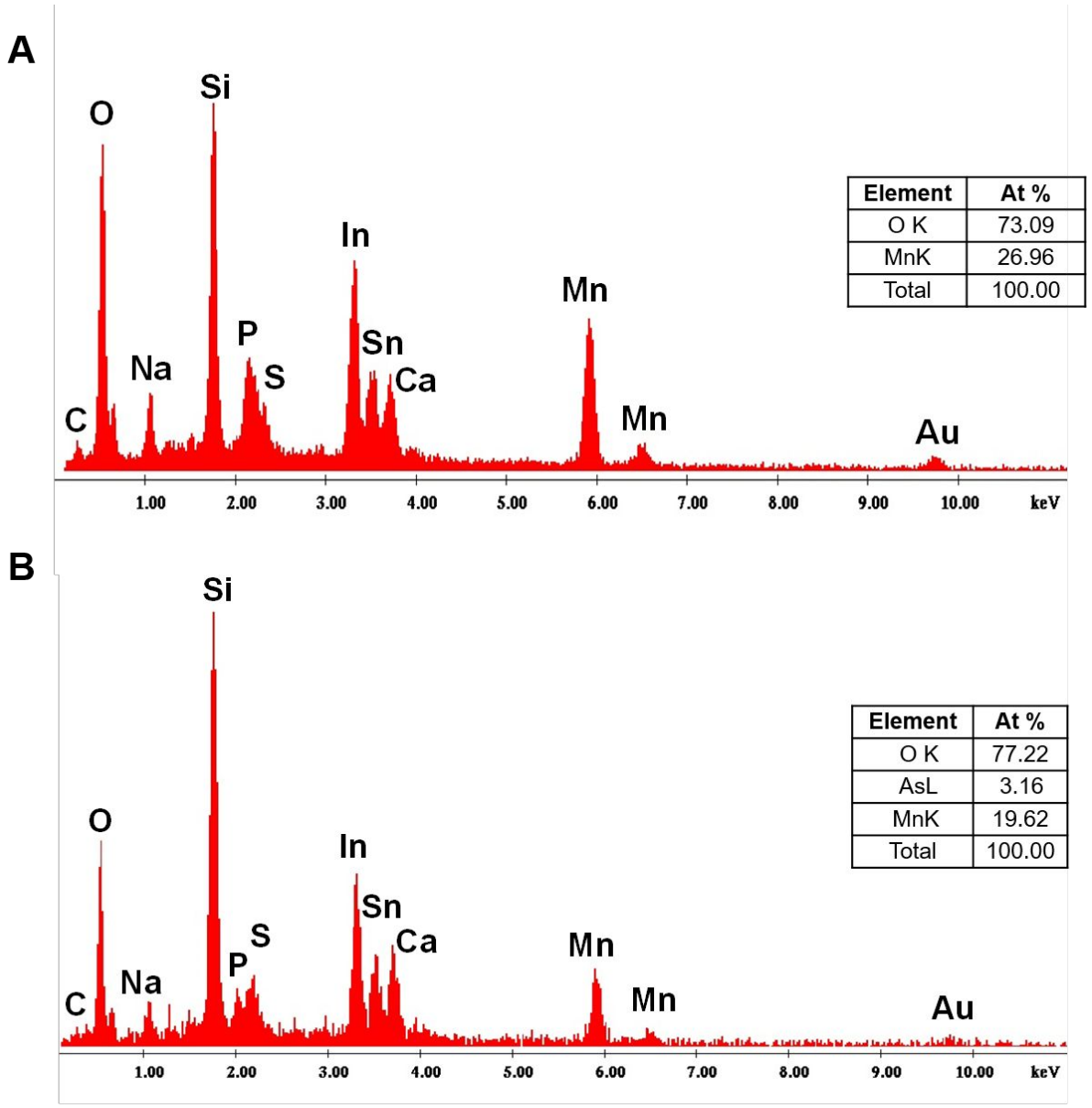

Figure S4. EDX spectra of **M3** electrode (A) before and (B) after As^{3+} sensing. Inset shows the element analysis. The change in Atomic % of Mn is attributed to the loss of Mn ions from the parent material by dissolution into the electrolyte during LSSV stripping of As^{3+}. Sn and In are from the substrate used.

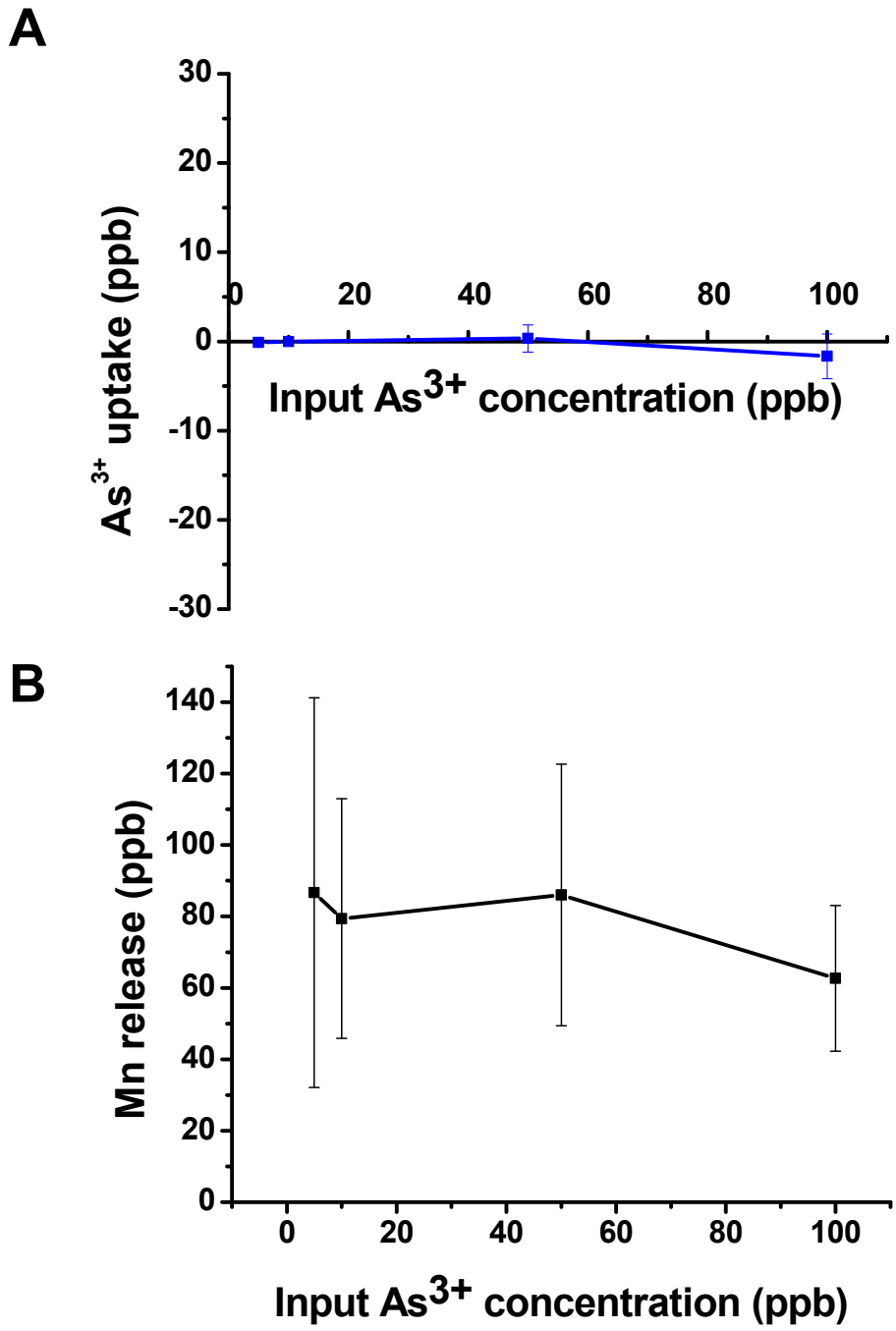

Figure S5: ICP-MS data of electrode **M3** for change in the (A) arsenic and (B) manganese ion concentrations in the electrolyte due to LSSV. The data is recorded with three different **M3** electrodes.

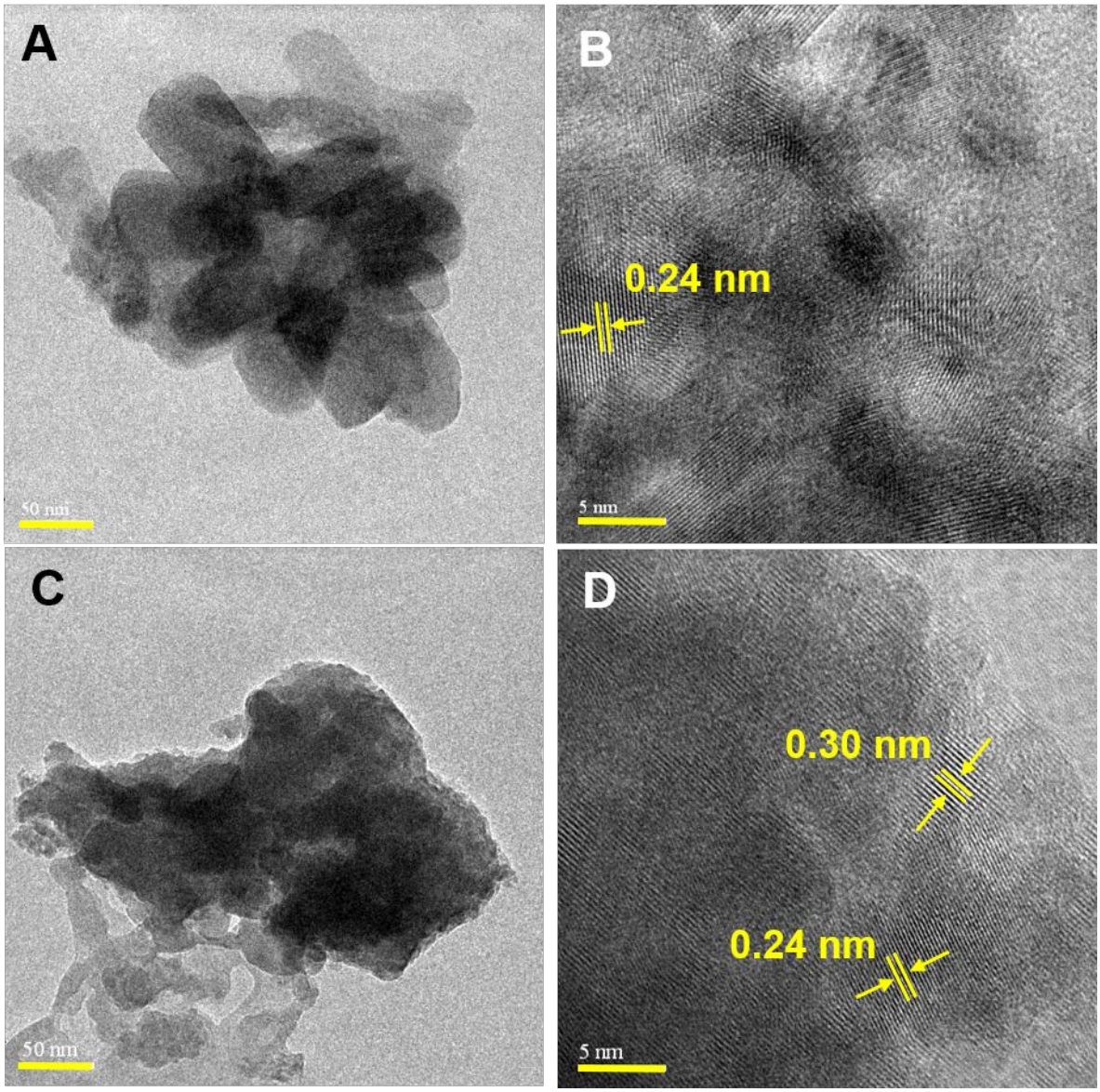

Figure S6. HRTEM micrographs of MnO_x from electrode **M1** (A and B) as-prepared and (C and D) after As^{3+} sensing. (A) Aggregated nanorod-like structures. (B) corresponding lattice spacing of ~0.24 nm. (C) Sheets of MnO_x. (D) corresponding lattice spacing of 0.24 and 0.30 nm. The scale bars are 50 nm for A and C, and 5 nm for B and D.

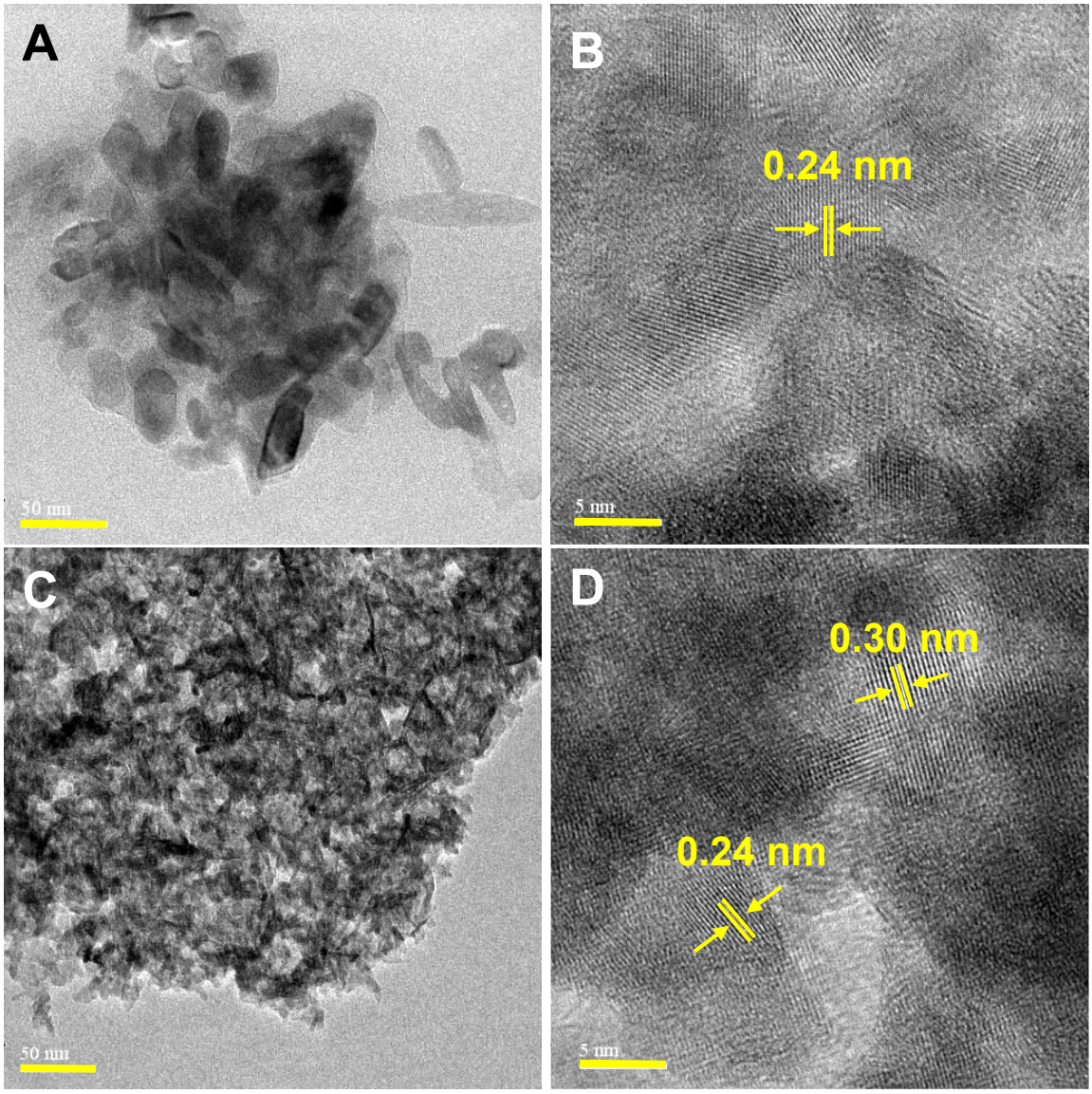

Figure S7. HRTEM micrographs of MnO_x from electrode **M2** (A and B) as-prepared and (C and D) after As^{3+} sensing. (A) Nanorod-like structures with their corresponding lattice spacing of ~0.24 nm in (B). (C) Crumpled paper-like morphology of MnO_x with lattice spacing of 0.24 and 0.30 nm in (D). The scale bars are 50 nm for A and C, and 5 nm for B and D.

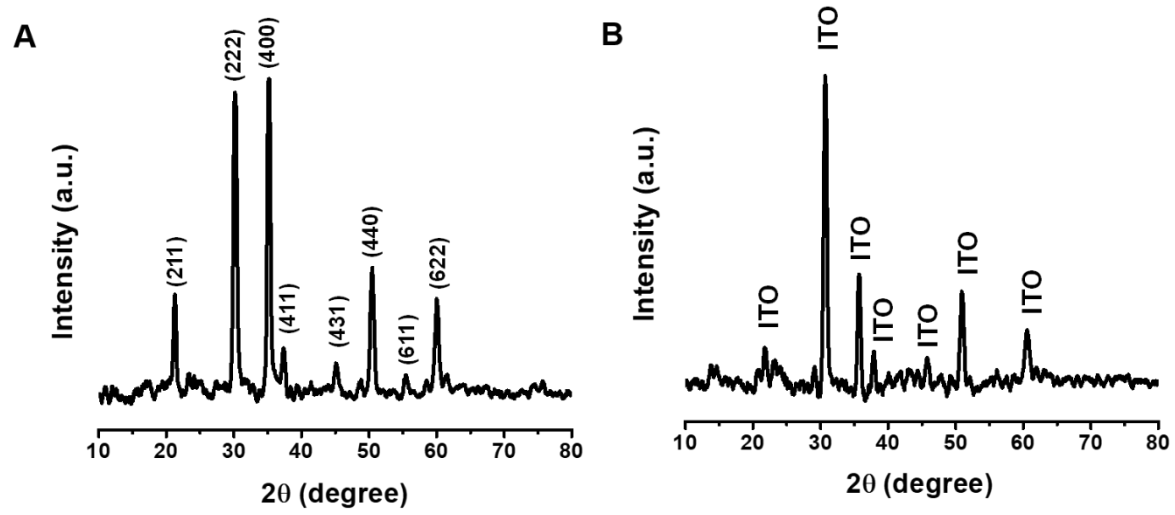

Figure S8. XRD patterns of (A) bare ITO glass substrate (JCPDS file no: 71-2194) and (B) control experiment on electrode **M3** involving LSSV in DI water and PBS electrolyte followed by washing with DI water. All peaks in B belong to ITO substrate, no additional peaks were observed.

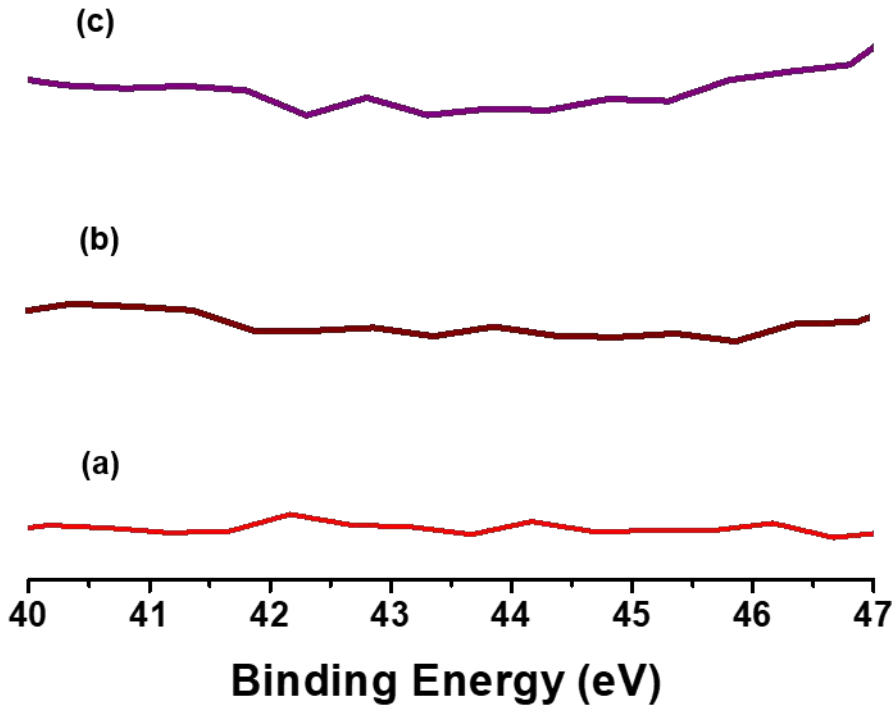

Figure S9. XPS spectra of As 3d region for electrode **M3**. (a), (b) and (c) correspond to bare ITO, before sensing and after sensing, respectively. Absence of As peak in (c) indicates that arsenic is not bound to the electrode surface after sensing.

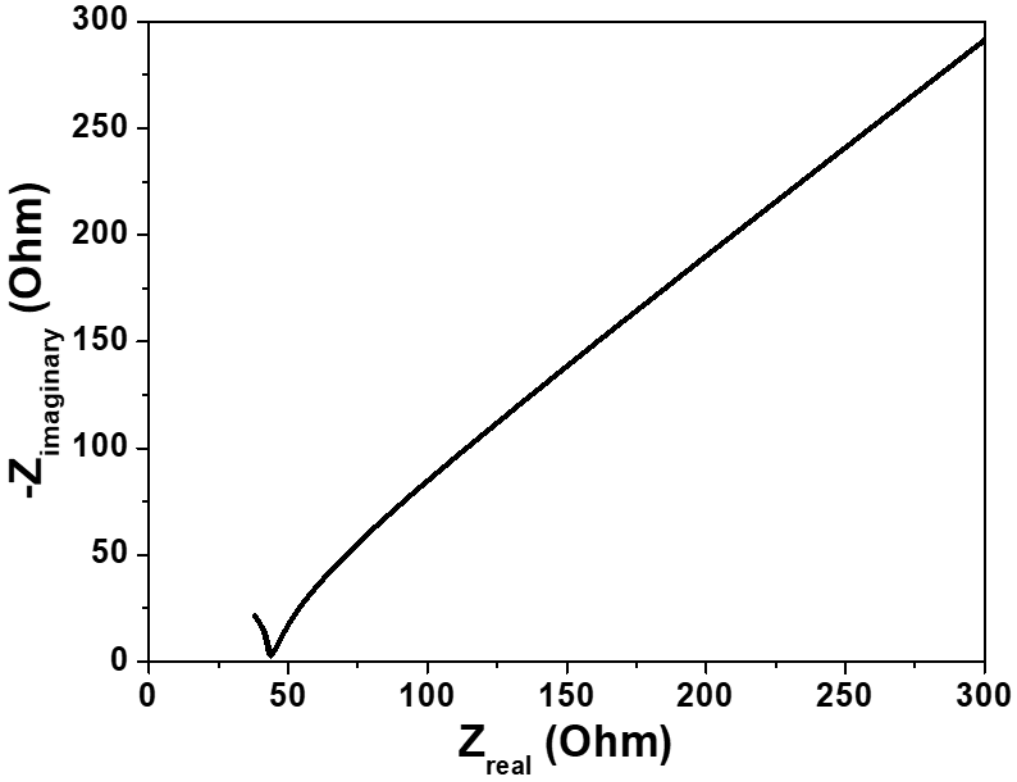

Figure S10. Nyquist plot of electrochemical impedance spectra for bare ITO glass substrate in PBS electrolyte (pH ~ 7.4).

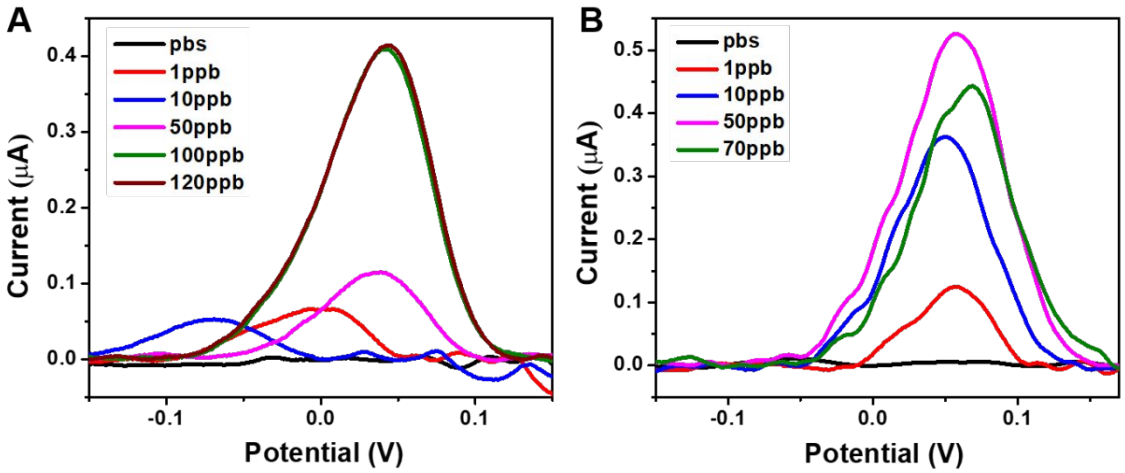

Figure S11. Electrochemical arsenite sensing response by MnO_x/ITO electrodes prepared at different CV voltage-windows: (A) **M1** and (B) **M2**.

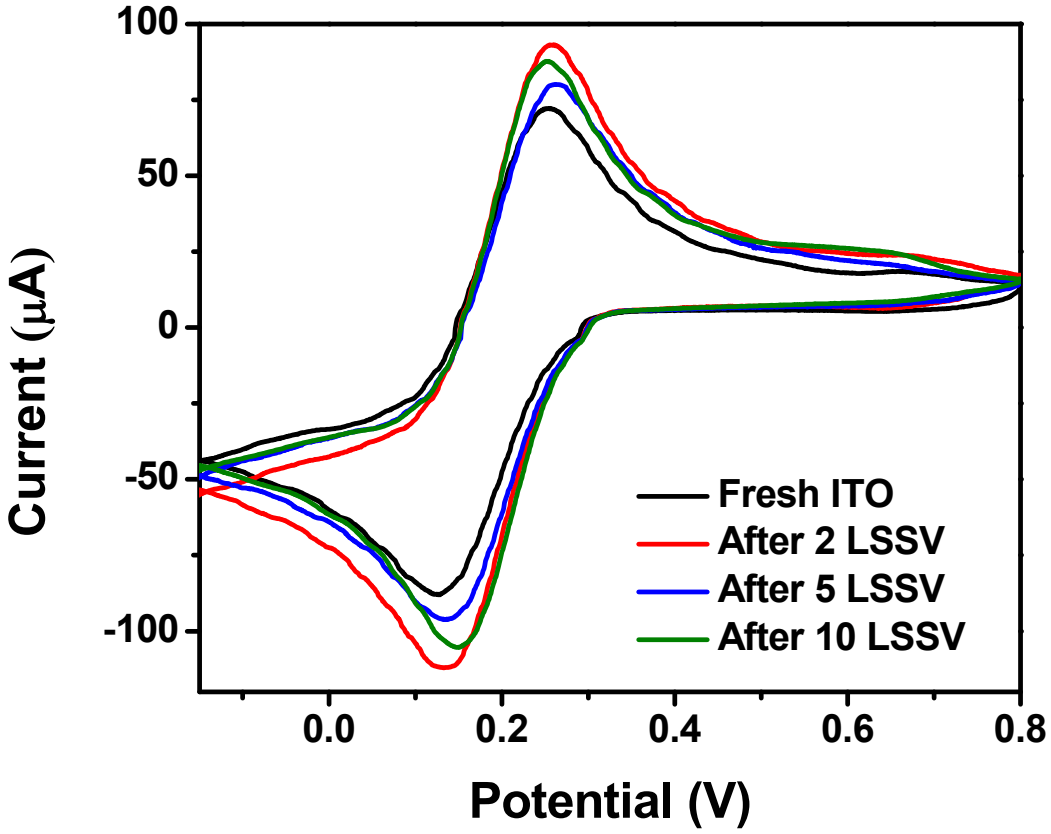

Figure S12. Cyclic voltammogram of bare ITO in 32.6 μM of potassium ferricyanide ($K_3Fe(CN)_6$) and 3.2 mM potassium chloride (KCl) as supporting electrolyte after performing LSSV at optimized parameters.

Calculation of LOD

The theoretical limit of detection (LOD) was calculated using the following formulae.[2]

LOB was estimated by measuring replicates of a blank sample and calculating both mean value and standard deviation (SD).

Limit of blank (LOB) = Mean blank + z-score × standard deviation of blank sample [1]

$= 1.32 \times 10^{-8} + 1.645 \times 4.15 \times 10^{-8}$

$= 8.146 \times 10^{-8}$

Theoretical Limit of detection (LOD) = LOB + z-score × (standard deviation of measured lowest concentration of sample) [2]

$= 8.146 \times 10^{-8} + 1.645 \times 0.0072$

$= 0.01195$ ppb

≈ 0.012 ppb

The z-score in Equations 1 and 2 is the number of standard deviations based on 90% confidence level. It is a statistical parameter.

References

1. Freitas, R. M.; Perilli, T. A. G.; Ladeira, A. C. Q. Oxidative Precipitation of Manganese from Acid Mine Drainage by Potassium Permanganate. *J. Chem.* **2013**, *2013*, 1–8.
2. Armbruster, D. A.; Pry, T. Limit of Blank, Limit of Detection and Limit of Quantitation. *Clin. Biochem. Rev.* **2008**, *29* (August), 49–52.